



Cite this: *Soft Matter*, 2019, 15, 5282

Mutualistic benefit in the self-sorted co-aggregates of *peri*-naphthoindigo and a 4-amino-1,8-naphthalimide derivative†

Rashmi Jyoti Das and Kingsuk Mahata *

Photoluminescence enhancement for all the members of a self-sorted co-aggregate was observed for the first time by successfully amalgamating AIEE and social self-sorting. Intermolecular H-bonding and π - π stacking were utilised to prepare several co-aggregates of *peri*-naphthoindigo (PNI) and a 4-amino-1,8-naphthalimide derivative dye, NH₂-NMI. In the heteromeric aggregates, photoluminescence intensities were increased by 28% for the imide and more than 400% for PNI. Due to spectral overlap between the emission of the imide and the absorption of PNI, energy transfer took place from the former to the latter. The heteromeric aggregates are dual emissive and the relative intensities of the emissions can easily be tuned by varying the stoichiometry of the dyes.

Received 4th March 2019,
Accepted 6th June 2019

DOI: 10.1039/c9sm00454h

rsc.li/soft-matter-journal

Introduction

Social self-sorting¹ or high fidelity non-self-recognition is a universal phenomenon that has multifaceted appearances in Nature. In chemistry, social self-sorting is defined as a process in which two or more different molecules prefer to assemble with other(s) instead of themselves. Such a specific co-assembly process provides an opening to structural diversity in the resultant aggregate(s). Unsurprisingly, social self-sorting has been a topic of research among scientists over the last few decades.^{1–5} The principle has been exploited to fabricate a wide variety of multi-component complex molecular architectures.^{2–7} Considering structural diversity, the research in social self-sorting has been quite successful. But, the functional aspect of the self-sorting algorithm is still very inadequate. Only in recent years, Schmittel⁸ and others⁹ utilised the sorting protocol to assemble various molecular machines. The concept of self-sorting has also been extended to molecular cybernetics¹⁰ and light emitting materials. In an exciting paper, Stang *et al.* showed that the photoluminescence property of a molecule was significantly enhanced in heteromeric aggregates compared to the monomeric form.¹¹ Similar observations were reported by a few other groups.^{12,13} These examples are promising, but the numbers are still very low. Furthermore, there is no example where photoluminescence intensities have been increased for all the components of co-aggregates prepared by social self-sorting,

although in social networking practiced in Nature, every participating member benefits.¹⁴ Molecular social self-sorting thus requires additional dimensions to enhance its diversity and application potential.

Photoluminescence enhancement of a molecule occurs when contributions from nonradiative decay pathways are reduced. This is normally done by imposing a restriction in molecular rotation and/or vibration through aggregation or crystallisation. Photoluminescence enhancement due to restriction in intramolecular motion is a well-known phenomenon and the concept has been studied extensively over the last two decades.^{15,16} The principle of aggregation-induced enhanced emission (AIEE) has been utilised in diverse areas including bioscience, energy, medicine, optics and electronics.¹⁷ Judicious application of the AIEE concept in social self-sorting would lead to enhancement of emission of all the entities involved in a co-assembly. However, amalgamation of these two independent concepts needs masterful design. Every component involved in a co-aggregate generated *via* the social self-sorting process should have provision for photoluminescence enhancement in the aggregate. Successful installation of the two independent concepts would give another benefit in terms of Förster resonance energy transfer (FRET), if there is spectral overlap between the absorbance of one component and emission of the other.

To observe a photoluminescence enhancement in a self-sorted multi-component co-assembly, we decided to use *peri*-naphthoindigo (PNI) as one partner (Chart 1). PNI is an ambipolar dye in which four functional groups are sandwiched between two naphthalene rings *via peri*-positions. Although the structure of the dye was proposed several decades ago in a patent,¹⁸ its synthesis was reported recently for the first time by us.¹⁹ Unlike the anticipated

Department of Chemistry, Indian Institute of Technology Guwahati, Assam 781039, India. E-mail: kingsuk@iitg.ac.in

† Electronic supplementary information (ESI) available: NMR, absorption, and photoluminescence spectra, FESEM images. See DOI: 10.1039/c9sm00454h

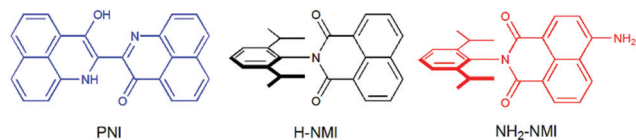


Chart 1 Structures of molecules used for co-assembly processes.

diketo isomer,^{18,20} PNI exists in mono-enol form. Due to the special structural feature, PNI has potential to show emission enhancement in the aggregated form. Another reason to choose PNI is its unique photophysical properties. The dye emits in the near-infrared region with the maximum at 736 nm (in CHCl₃). Enhancement of emission in the bio-optical region is very much in demand for various applications.²¹ PNI also absorbs in a broad region, which gives it a good chance to fulfil criteria for the FRET process. The second partner for the co-assembly process must be complementary to PNI. Accordingly, we chose two naphthalene monoimide based dyes, H-NMI and NH₂-NMI (Chart 1). In this communication, we have explored various self-sorting processes involving the dyes and reported for the first time the mutual enhancement of emission in the self-sorted co-aggregates of NH₂-NMI and PNI. In the heteromeric aggregates of the two dyes, emissions were increased by more than 5 times for PNI and 1.28 fold for the imide. Additionally, energy transfer took place from the imide to PNI.

Results and discussion

We first explored the self-assembly process of PNI by varying solvent polarity as well as concentration. PNI was found to be in the aggregated form in DMSO only at a very high concentration ($c \approx 20 \text{ mmol L}^{-1}$). Switching from the monomer to the aggregate could be detected using ¹H NMR spectroscopy (Fig. S3, ESI[†]). But, it was not possible to observe the change by UV-vis spectroscopy (Fig. S7, ESI[†]). The high concentration demand limited our scope for photophysical property investigations. To overcome this problem, we considered a solvent system in which self-assembly is possible even at a very low concentration. As PNI is an ambipolar dye, its aggregation property can easily be tuned by changing the solvent polarity. The functional groups in the molecule do not like nonpolar solvents, while naphthalene rings avoid polar solvents. We investigated the effect of increased polarity by dissolving the dye in DMSO and subsequently adding water into the solution. It was indeed possible to observe the self-assembly process at a very low concentration ($c \approx 5 \times 10^{-6} \text{ mol L}^{-1}$) in a mixture of DMSO and H₂O ($v/v = 1:9$). Aggregate formation in the solution was confirmed by UV-vis spectroscopy. A red shifted shoulder at 690 nm along with diminished molar extinction coefficient at the maximum (632 nm) proved the self-assembly process (Fig. S8, ESI[†]). To avoid unfavourable interactions between the hydrophobic naphthalene rings of PNI and water molecules, aggregation occurred even at a low concentration. Emission of PNI was found to be quenched completely in the DMSO–water mixture. Vibrational energy transfer to water molecules probably diminished the emission. As our goal was to observe a photoluminescence enhancement,

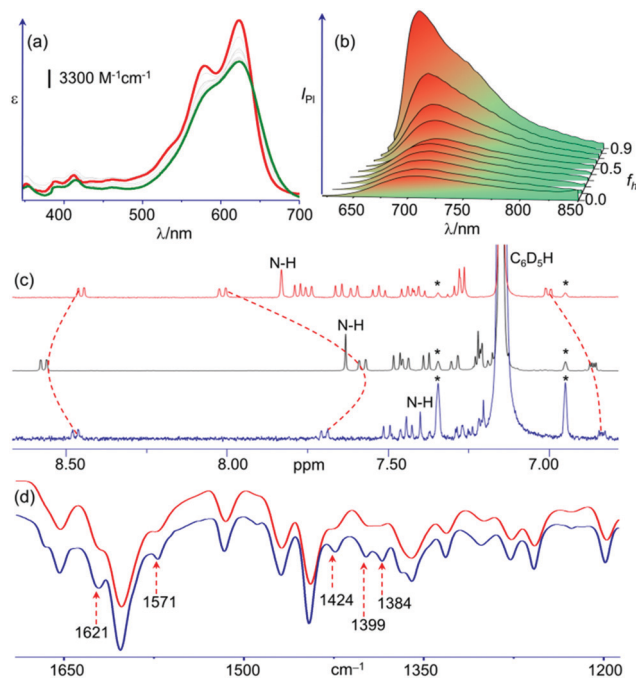


Fig. 1 (a) Absorption spectra of PNI in THF (green) and in a mixture (red) of THF/*n*-hexane ($v/v = 1:9$). (b) Photoluminescence (PI) spectra of PNI in THF and in mixtures of THF and *n*-hexane. Emission maximum gradually blue shifted with an increase in f_h . (c) ¹H NMR (400 MHz, 295 K) spectra of PNI in C₆D₆ (black), THF/C₆D₆ (red) and *n*-hexane/C₆D₆ (blue); satellite peaks are marked with asterisks. (d) Comparison of IR spectra of PNI monomer (red) and aggregate (blue).

a different solvent combination was needed. In the next set of experiments, we reduced the polarity of the solvent by gradual addition of *n*-hexane to a THF solution of PNI and the process was investigated using UV-vis spectroscopy. The absorption spectra became vibronically resolved when the volume fraction of *n*-hexane (f_h) reached 0.9 (Fig. 1a). Additionally, there was an increase in molar extinction coefficient at the absorption maximum. A restriction in intramolecular motion through aggregation possibly caused such changes. UV-vis absorption property investigations (Fig. S12, ESI[†]), at different concentrations ($1 \times 10^{-6} \text{ mol L}^{-1}$ to $1 \times 10^{-3} \text{ mol L}^{-1}$) in THF/*n*-hexane ($v/v = 1:9$), suggested the formation of larger aggregates at higher concentration, marked by a decreased molar extinction coefficient. Unlike the studies mentioned earlier, the PNI-aggregate was found to be emissive in a mixture of THF and *n*-hexane. A comparison of photoluminescence properties of PNI in different fractions of THF and *n*-hexane is shown in Fig. 1b. With an increase in f_h , emission intensity gradually increased, and at $f_h = 0.9$, a more than 6 fold enhancement was recorded. The observations confirmed the aggregation-induced photoluminescence enhancement of PNI. In addition to the amplified photoluminescence, there was a gradual hypsochromic shift of the emission maximum with an increase in f_h . Such a decrease in Stokes shift also supported rigidification of the structure *via* aggregation. The self-assembly process of PNI was further established from ¹H NMR investigations. We measured the ¹H NMR spectra of PNI in three different solvent systems, C₆D₆: THF ($v/v = 1:2$), C₆D₆ and C₆D₆: *n*-hexane ($v/v = 1:1$). Almost all the

proton signals changed with variation in polarity (Fig. 1c). For example, the N–H signal experienced an upfield shift of 0.43 ppm going from the most polar solvent combination C₆D₆-THF to the least polar system C₆D₆/*n*-hexane. All these observations confirmed the aggregation process of PNI. The self-assembly process was further corroborated using infrared (IR) spectroscopy. For the same purpose, bulk solid and ordered aggregates of PNI were isolated by evaporating THF and THF/*n*-hexane (*v/v* = 1 : 9) solutions of the dye. The IR spectra of the two samples were notably different (Fig. 1d). Significant changes were observed at around 1384, 1399, 1424, 1571 and 1621 cm⁻¹. Peaks were broad in the bulk solid, but became sharp in the ordered aggregates. Powder X-ray diffraction (PXRD) patterns of the two different solids were compared to see the differences in intermolecular arrangement. The presence of more signals in the PXRD pattern (Fig. S6, ESI†) of the solid generated from THF/*n*-hexane (*v/v* = 1 : 9) confirmed the existence of highly ordered intermolecular arrangements *via* the self-assembly process. The nature of the morphology generated in the self-assembly process was investigated by field emission scanning electron microscopy (FESEM). The FESEM image of the aggregate on a surface, prepared by drop-casting a solution of PNI in THF/*n*-hexane (*v/v* = 1 : 9), showed the formation of well-defined microcrystalline cuboid architectures (Fig. 2). The height and width of the cuboids were found to be in the range of 50–500 nm. In length, the aggregates were extended up to several microns. The self-assembly process can be explained by considering intermolecular H-bond formation and subsequent stacking. With a decrease in solvent polarity, unfavorable interactions between the polar functional groups and non-polar solvents increased. To avoid the same, intermolecular H-bonding took place resulting in the formation of a one dimensional (1D) sheet-like morphology. The chromophore part was further masked by a brick wall type stacking of the sheets, producing 3D cuboid architectures. The overall process is summarised in Fig. 2.

Our next objective was to prepare a self-sorted co-aggregate of PNI and naphthalene monoimide H-NMI (Chart 1).²² In a two-component system, self-sorting is often enabled by installing steric control, which prevents homomeric aggregation of one and

forces the other partner to produce a heteromeric assembly.²³ We followed a similar strategy here. A bulky group was introduced into the imide position in H-NMI to prevent homomeric aggregate formation of the same. We checked the self-assembly potential of H-NMI in solution and monitored the process using UV-vis spectroscopy. The naphthalimide displayed absorption maximum at 343 nm in THF/*n*-hexane (*v/v* = 1 : 9) and the spectra remained the same even at various concentrations (Fig. S10, ESI†), suggesting the inability of H-NMI towards self-aggregation in the specified solvent system. We then investigated the co-self-assembly process of the imide with PNI. To obtain the heteromeric aggregate, PNI and H-NMI were mixed in a 10 : *n* (*n* = 1, 2, ..., 5) molar ratio in THF, followed by addition of *n*-hexane to make the final *f_h* 0.9. Similar to the self-aggregation of PNI, the absorption spectrum of the co-assembly process was found to be vibronically resolved (Fig. 3a). But, a major change was noticed between 300 and 450 nm (Fig. 3a). Besides an increase in molar absorptivity near the absorption maximum of H-NMI, there occurred significant changes around the absorption of PNI. Furthermore, the absorption spectrum of the co-assembly process appeared to be different than the mathematical summation of the spectra of self-assembled PNI and monomeric H-NMI, which confirmed the formation of a heteromeric aggregate and excluded the possibility of a mixture of monomeric H-NMI and the homomeric PNI-aggregate. A FESEM image (Fig. 3b) of the co-assembly process shows a ribbon-shaped aggregate, which was generated *via* sandwiching of H-NMI into the 1D sheets of PNI (Fig. S27, ESI†). The heteromeric aggregates were found to be several hundred micrometres long. The uniform morphology confirmed the exclusive formation of heteromeric aggregates. Photoluminescence of PNI in the co-assembly process was increased in a similar fashion as observed in the case of homomeric aggregation (Fig. S16, ESI†). The heteromeric aggregates can be prepared either in a single step, as mentioned above, or in a stepwise manner by adding NMI to the self-assembled PNI in THF/*n*-hexane (*v/v* = 1 : 9). The outcomes were found to be the same in both cases. The naphthalimide remained non-emissive in the monomeric form as well as in the aggregate. Because of the very rigid structure of H-NMI, there was no scope for emission enhancement and the outcome was indeed unsurprising. To observe an emission enhancement for every component, modification was needed for the imide.

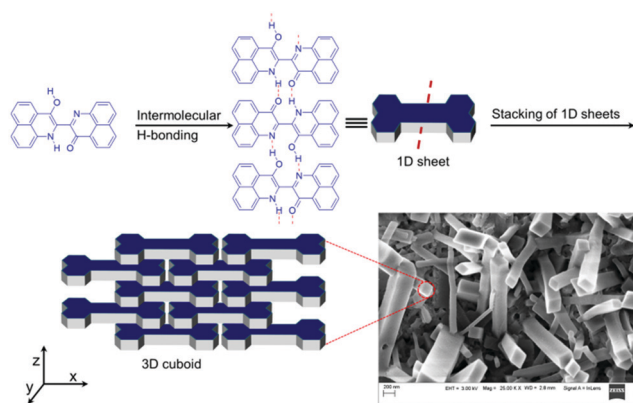


Fig. 2 Stepwise self-assembly process of PNI along with FESEM image of the aggregates.

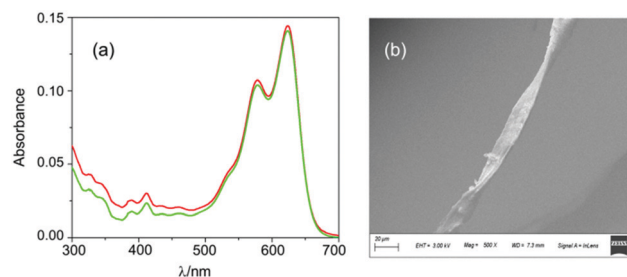


Fig. 3 (a) Experimental (red) and hypothetical (green) absorption spectra of a co-aggregate of PNI and H-NMI (10 : 2 molar ratio). Hypothetical spectrum was calculated by adding absorption spectra of homomeric aggregate of PNI and monomeric H-NMI in 10 : 2 molar ratio. (b) FESEM image of heteromeric aggregate of PNI and H-NMI.

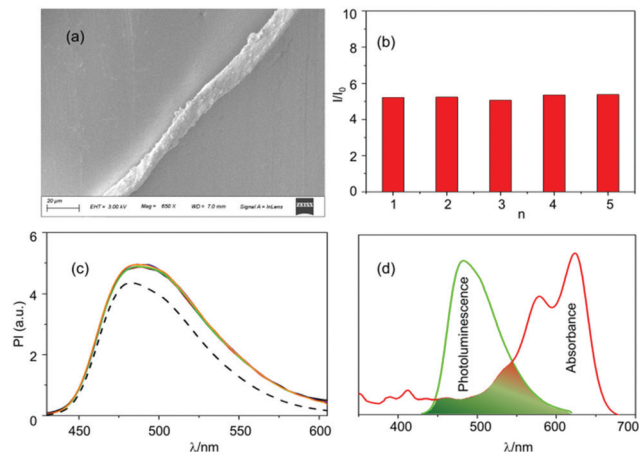


Fig. 4 (a) FESEM image of heteromeric aggregate of PNI and $\text{NH}_2\text{-NMI}$. The sample was prepared by mixing PNI and $\text{NH}_2\text{-NMI}$ in a 10 : 1 molar ratio. (b) Photoluminescence enhancement of PNI in the co-aggregates ($\text{PNI}/\text{NH}_2\text{-NMI} = 10 : n$). (c) Photoluminescence spectra of $\text{NH}_2\text{-NMI}$ in monomer (black, dashed) and in co-aggregates (coloured, solid) in THF/ n -hexane ($v/v = 1 : 9$). (d) Spectral overlap between the emission spectrum of $\text{NH}_2\text{-NMI}$ (green) and the absorption spectrum of PNI (red).

To achieve our final goal, the mutual enhancement of emission for every component in a social self-sorting process, we introduced an amino group at the 4-position of naphthalimide and prepared $\text{NH}_2\text{-NMI}$ (Chart 1).²⁴ The amino group was incorporated for two reasons. Restriction in rotation of the amino group might give enhanced emission in the resultant co-aggregate. Spectral overlap between the emission of $\text{NH}_2\text{-NMI}$ and the absorption of PNI would give a chance for energy transfer. Concentration dependent studies of the imide did not result in any change in absorption spectra (Fig. S11, ESI†). Investigation of the co-assembly process of $\text{NH}_2\text{-NMI}$ with PNI revealed a similar outcome, *i.e.* the formation of ribbon-shaped heteromeric aggregates (Fig. 4a) *via* self-sorting. Time-resolved photoluminescence spectroscopy revealed an improved lifetime, from 8.24 ns in the monomer to 8.84 ns in the co-assembled aggregate, for the imide dye. A comparative study of photoluminescence intensity showed a 1.28-fold enhancement for $\text{NH}_2\text{-NMI}$ and more than 5-fold enhancement for PNI in the co-assembled aggregate (Fig. 4b and c). We then focused on the FRET process in the co-aggregate as there is spectral overlap between the emission of the imide and the absorption of PNI (Fig. 4d). The energy transfer process was investigated by exciting at the absorption maximum of $\text{NH}_2\text{-NMI}$ and recording the steady-state emission of PNI. It was indeed possible to detect enhanced emission of PNI at 657 nm after excitation of the heteromeric aggregate at the absorption maximum of the imide (410 nm). It is necessary to mention that the homomeric aggregate of PNI shows weak emission after excitation at 410 nm. This observation proved the successful energy transfer from the imide to PNI (Fig. S19, ESI†). However, the FRET process was not quantitative and dual emission was observed after excitation at 410 nm. The relative intensities of the dual emission can easily be tuned simply by changing the stoichiometry of the dyes (Fig. S20, ESI†).

Conclusions

In summary, we have successfully amalgamated AIEE and social self-sorting. Both the imides, H-NMI and $\text{NH}_2\text{-NMI}$, can exclusively form heteromeric aggregates with PNI *via* a sorting process. But, the perfect pair for the merger of AIEE and social self-sorting was $\text{NH}_2\text{-NMI}$ and PNI. Photoluminescence intensities were increased by up to 28% for the imide and more than 400% for PNI in the co-assemblies of the two dyes. Although PNI can exhibit AIEE alone, $\text{NH}_2\text{-NMI}$ needs support from PNI to enhance its photoluminescence intensity. Due to spectral overlap between the emission of $\text{NH}_2\text{-NMI}$ and the absorption of PNI, energy transfer took place from the former dye to the latter. This model can be useful for efficient energy harvesting due to greater coverage of the solar spectrum *via* multi-component assembly and energy funneling.²⁵ The dual emissive nature of the co-aggregates of PNI and $\text{NH}_2\text{-NMI}$ will be useful for various photoluminescence-based applications.

Conflicts of interest

The authors declare no competing financial interests.

Acknowledgements

We thank the Science and Engineering Research Board, Government of India for financial support (SB/FT/CS-184/2013). RJD thanks IIT Guwahati for her doctoral fellowship. We are grateful to the Department of Chemistry and the Central Instrumental Facility, Indian Institute of Technology Guwahati, for various instrumental facilities.

References

- (a) A. Wu and L. Isaacs, *J. Am. Chem. Soc.*, 2003, **125**, 4831–4835; (b) L. Isaacs, *Acc. Chem. Res.*, 2014, **47**, 2052–2062.
- (a) P. Mukhopadhyay, A. Wu and L. Isaacs, *J. Org. Chem.*, 2004, **69**, 6157–6164; (b) N. Tomimasu, A. Kanaya, Y. Takashima, H. Yamaguchi and A. Harada, *J. Am. Chem. Soc.*, 2009, **131**, 12339–12343; (c) W. Jiang, Q. Wang, I. Linder, F. Klautzsch and C. A. Schalley, *Chem. – Eur. J.*, 2011, **17**, 2344–2348; (d) M. J. Mayoral, C. Rest, J. Schellheimer, V. Stepanenko and G. Fernández, *Chem. – Eur. J.*, 2012, **18**, 15607–15611; (e) L. Li, H.-Y. Zhang, J. Zhao, N. Li and Y. Liu, *Chem. – Eur. J.*, 2013, **19**, 6498–6506; (f) K. Han, D. Go., T. Tigges, K. Rahimi, A. J. C. Kuehne and A. Walther, *Angew. Chem., Int. Ed.*, 2017, **56**, 2176–2182; (g) S. Díaz-Cabrera, Y. Dorca, J. Calbo, J. Aragón, R. Gómez, E. Ortí and L. Sánchez, *Chem. – Eur. J.*, 2018, **24**, 2826–2831; (h) H. M. Coubrough, S. C. C. van der Lubbe, K. Hetherington, A. Minard, C. Pask, M. J. Howard, C. F. Guerra and A. J. Wilson, *Chem. – Eur. J.*, 2019, **25**, 785–795.
- (a) R. Joseph, A. Nkrumah, R. J. Clark and E. Masson, *J. Am. Chem. Soc.*, 2014, **136**, 6602–6607; (b) T. Rama, A. Blanco-Gómez, I. Neira, O. Domarco, M. D. García, J. M. Quintela and C. Peinador, *Chem. – Eur. J.*, 2017, **23**, 16743–16747;

- (c) Y.-S. Wang, T. Feng, Y.-Y. Wang, F. E. Hahn and Y.-F. Han, *Angew. Chem., Int. Ed.*, 2018, **57**, 15767–15771; (d) M. Raeisi, K. Kotturi, I. del Valle, J. Schulz, P. Dornblut and E. Masson, *J. Am. Chem. Soc.*, 2018, **140**, 3371–3377.
- 4 (a) S. Klotzbach and F. Beuerle, *Angew. Chem., Int. Ed.*, 2015, **54**, 10356–10360; (b) D. Beaudoin, F. Rominger and M. Mastalerz, *Angew. Chem., Int. Ed.*, 2017, **56**, 1244–1248.
- 5 (a) M. M. Safont-Sempere, G. Fernández and F. Würthner, *Chem. Rev.*, 2011, **111**, 5784–5814; (b) L. E. Buerkle and S. J. Rowan, *Chem. Soc. Rev.*, 2012, **41**, 6089–6102; (c) M. L. Saha, S. Neogi and M. Schmittel, *Dalton Trans.*, 2014, **43**, 3815–3834; (d) Q. Ji, R. C. Lirag and O. Š. Miljanić, *Chem. Soc. Rev.*, 2014, **43**, 1873–1884; (e) Z. He., W. Jiang and C. A. Schalley, *Chem. Soc. Rev.*, 2015, **44**, 779–789; (f) W. M. Bloch and G. H. Clever, *Chem. Commun.*, 2017, **53**, 8506–8516; (g) N. Sinha and F. E. Hahn, *Acc. Chem. Res.*, 2017, **50**, 2167–2184; (h) L. R. Holloway, P. M. Bogie and R. J. Hooley, *Dalton Trans.*, 2017, **46**, 14719–14723; (i) F. Beuerle and B. Gole, *Angew. Chem., Int. Ed.*, 2018, **57**, 4850–4878; (j) M. Mastalerz, *Acc. Chem. Res.*, 2018, **51**, 2411–2422.
- 6 (a) A. Wu, A. Chakraborty, J. C. Fettinger, R. A. Flowers II and L. Isaacs, *Angew. Chem., Int. Ed.*, 2002, **41**, 4028–4031; (b) W. Jiang, H. D. F. Winkler and C. A. Schalley, *J. Am. Chem. Soc.*, 2008, **130**, 13852–13853; (c) K. Osowska and O. Š. Miljanić, *J. Am. Chem. Soc.*, 2011, **133**, 724–727; (d) S. Onogi, H. Shigemitsu, T. Yoshii, T. Tanida, M. Ikeda, R. Kubota and I. Hamachi, *Nat. Chem.*, 2016, **8**, 743–752; (e) H. A. M. Ardoña, E. R. Draper, F. Citossi, M. Wallace, L. C. Serpell, D. J. Adams and J. D. Tovar, *J. Am. Chem. Soc.*, 2017, **139**, 8685–8692; (f) P. Pramanik, D. Ray, V. K. Aswal and S. Ghosh, *Angew. Chem., Int. Ed.*, 2017, **56**, 3516–3520; (g) W. Drożdż, C. Bouillon, C. Kotras, S. Richeter, M. Barboiu, S. Clément, A. R. Stefankiewicz and S. Ulrich, *Chem. – Eur. J.*, 2017, **23**, 18010–18018; (h) E. R. Cross, S. Sproules, R. Schweins, E. R. Draper and D. J. Adams, *J. Am. Chem. Soc.*, 2018, **140**, 8667–8670.
- 7 (a) S. Ulrich and J.-M. Lehn, *J. Am. Chem. Soc.*, 2009, **131**, 5546–5559; (b) K. Mahata, M. L. Saha and M. Schmittel, *J. Am. Chem. Soc.*, 2010, **132**, 15933–15935; (c) A. M. Johnson and R. J. Hooley, *Inorg. Chem.*, 2011, **50**, 4671–4673; (d) M. L. Saha and M. Schmittel, *J. Am. Chem. Soc.*, 2013, **135**, 17743–17746; (e) T. K. Ronson, D. A. Roberts, S. P. Black and J. R. Nitschke, *J. Am. Chem. Soc.*, 2015, **137**, 14502–14512; (f) P. Howlader and P. S. Mukherjee, *Chem. Sci.*, 2016, **7**, 5893–5899.
- 8 (a) S. De, S. Pramanik and M. Schmittel, *Angew. Chem., Int. Ed.*, 2014, **53**, 14255–14259; (b) M. Schmittel, *Chem. Commun.*, 2015, **51**, 14956–14968; (c) S. K. Samanta, A. Rana and M. Schmittel, *Angew. Chem., Int. Ed.*, 2016, **55**, 2267–2272.
- 9 (a) P. Waelés, B. Riss-Yaw and F. Coutrot, *Chem. – Eur. J.*, 2016, **22**, 6837–6845; (b) L. Zhiquan, H. Xie, S. E. Border, J. Gallucci, R. Z. Pavlović and J. D. Badjić, *J. Am. Chem. Soc.*, 2018, **140**, 11091–11100.
- 10 M. Schmittel, *Isr. J. Chem.*, 2019, **59**, 197–208.
- 11 X. Yan, T. R. Cook, P. Wang, F. Huwang and P. J. Stang, *Nat. Chem.*, 2015, **7**, 342–348.
- 12 Q. Zhao, Y. Chen, S.-H. Li and Y. Liu, *Chem. Commun.*, 2018, **54**, 200–203.
- 13 (a) W.-C. Geng, Y.-C. Liu, Y.-Y. Wang, Z. Xu, Z. Zheng, C.-B. Yang and D.-S. Guo, *Chem. Commun.*, 2017, **53**, 392–395; (b) J.-Y. Chen, G. Kadam, A. Gupta, Anuradha, S. V. Bhosale, F. Zheng, C.-H. Zhou, B.-H. Jia, D. S. Dalal and J.-L. Li, *Chem. – Eur. J.*, 2018, **24**, 14668–14678.
- 14 D. Umberson and J. K. Montez, *J. Health Soc. Behav.*, 2010, **51**(suppl), S54–S66.
- 15 J. Luo, Z. Xie, J. W. Y. Lam, L. Cheng, H. Chen, C. Qiu, H. S. Kwok, X. Zhan, Y. Liu, D. Zhu and B. Z. Tang, *Chem. Commun.*, 2001, 1740–1741.
- 16 (a) Y. Hong, J. W. Y. Lam and B. Z. Tang, *Chem. Commun.*, 2009, 4332–4353; (b) Z. He, C. Ke and B. Z. Tang, *ACS Omega*, 2018, **3**, 3267–3277; (c) H.-T. Feng, Y.-X. Yuan, J.-B. Xiong, Y.-S. Zheng and B. Z. Tang, *Chem. Soc. Rev.*, 2018, **47**, 7452–7476.
- 17 (a) Z. Zhao, J. W. Y. Lam and B. Z. Tang, *J. Mater. Chem.*, 2012, **22**, 23726–23740; (b) Z. Chi, X. Zhang, B. Xu, X. Zhou, C. Ma, Y. Zhang, S. Liu and J. Xu, *Chem. Soc. Rev.*, 2012, **41**, 3878–3896; (c) J. Mei, Y. Hong, J. W. Y. Lam, A. Qin, Y. Tang and B. Z. Tang, *Adv. Mater.*, 2014, **26**, 5429–5479; (d) J. L. Banal, B. Zhang, D. J. Jones, K. P. Ghiggino and W. W. H. Wong, *Acc. Chem. Res.*, 2017, **50**, 49–57; (e) F. Hu, S. Xu and B. Liu, *Adv. Mater.*, 2018, **30**, 1801350; (f) G. Feng and B. Liu, *Acc. Chem. Res.*, 2018, **51**, 1404–1414; (g) J. Li and K. Pu, *Chem. Soc. Rev.*, 2019, **48**, 38–71.
- 18 R. A. Nathan, R. E. Schwerzel, A. H. Adelman and R. E. Wyant, *US Pat.*, 4004572, 1977.
- 19 R. J. Das and K. Mahata, *Org. Lett.*, 2018, **20**, 5027–5031.
- 20 S.-F. Zhang, X.-K. Chen, J.-X. Fan and A.-M. Ren, *Org. Electron.*, 2015, **24**, 12–25.
- 21 (a) J. O. Escobedo, O. Rusin, S. Lim and R. M. Strongin, *Curr. Opin. Chem. Biol.*, 2010, **14**, 64–70; (b) L. Yuan, W. Lin, K. Zheng, L. He and W. Huang, *Chem. Soc. Rev.*, 2013, **42**, 622–661; (c) Z. Guo, S. Park, J. Yoon and I. Shin, *Chem. Soc. Rev.*, 2014, **43**, 16–29; (d) H. Chen, B. Dong, Y. Tang and W. Lin, *Acc. Chem. Res.*, 2017, **50**, 1410–1422.
- 22 (a) T. Weil, E. Reuther and K. Müllen, *Angew. Chem., Int. Ed.*, 2002, **41**, 1900–1904; (b) F. Nolde, J. Qu, C. Kohl, N. G. Pschirer, E. Reuther and K. Müllen, *Chem. – Eur. J.*, 2005, **11**, 3959–3967; (c) W. Zhang, Y. Xu, M. Hanif, S. Zhang, J. Zhou, D. Hu, Z. Xie and Y. Ma, *J. Phys. Chem. C*, 2017, **121**, 23218–23223.
- 23 K. Mahata and M. Schmittel, *J. Am. Chem. Soc.*, 2009, **131**, 16544–16554, and references cited therein.
- 24 A. Boehm, H. Schmeisser, S. Becker and K. Müllen, *Ger. Offen.*, DE19940708 A1 20010301, 2001.
- 25 (a) R. Ziessel and A. Harriman, *Chem. Commun.*, 2011, **47**, 611–631; (b) C. Kreisbeck and A. Aspuru-Guzik, *Chem. Sci.*, 2016, **7**, 4174–4183; (c) T. Mirkovic, E. E. Ostroumov, J. M. Anna, R. van Grondelle, Govindjee and G. D. Scholes, *Chem. Rev.*, 2017, **117**, 249–293.